



Reconstruction of landslide model from ERT, geotechnical, and field data, Nargeschal landslide, Iran

Sadegh Rezaei¹ · Issa Shooshpasha¹ · Hamed Rezaei²

Received: 19 January 2018 / Accepted: 16 July 2018 / Published online: 1 August 2018
© Springer-Verlag GmbH Germany, part of Springer Nature 2018

Abstract

Landslides are natural hazards that cause severe casualties and financial losses. There are various methods used to analyze landslides; among these, geotechnical and geophysical methods are widely used due to their accuracy and low cost, respectively. In this study, 2D electrical resistivity tomography (ERT) surveys, geotechnical, and field data are used to define the subsurface structure and the geometry of the Nargeschal landslide. To determine the most appropriate array, ERT measurements were performed by Wenner-alpha (Wa), Wenner-Schlumberger (WS), and dipole-dipole (DD) arrays. Furthermore, the relationship between electrical resistivity with change in the degree of saturation and landslide hydrology was investigated by completing multiple surveys at the same location, at different times. Landslide 3D geometry and hydrology were identified by ERT results. Moreover, geotechnical data was used to investigate the Nargeschal landslide and to interpret the ERT pseudo sections. The data from boreholes were used to constrain the depth and consequently the resistivity range that characterize the basal slip surface of the landslide in the ERT pseudo sections. The results of geotechnical investigations indicated that the landslide material had moisture content very close to the plastic limit, with a higher clay fraction and low shear strength at the slip surface. Finally, it must be noted that the simultaneous use of the ERT survey, geotechnical methods, and field investigations led to a complete and accurate characterization of the Nargeschal landslide.

Keywords Landslide · Electrical resistivity tomography (ERT) · Geotechnical investigation · Slip surface geometry · Hydrology

Introduction

Landslides annually claim thousands of lives and result in severe financial losses because of the damage to human structures and other utilities. Numerous factors cause landslides, including earthquakes, heavy precipitation, volcanic mechanisms, and human activities, such as excavation on steep slopes, etc. Depending on the characteristics of the involved material, landslides usually occur on steeper slopes (over an angle of 25°) and weak layers (saturated clay soil with weak shear strength) (Hibert et al. 2012; Akpan et al. 2015). Sometimes, a landslide can bury a city or village completely

under the failed mass, causing irrecoverable damage (e.g., the burial of the Yungay village in Peru due to a landslide in 1970) (Kramer 1996). Therefore, in order to reduce the risk associated with landslides, it is essential to have a complete knowledge of their geometry, hydrology, material properties, and ongoing kinematics (Guerriero et al. 2016).

A comprehensive reconstruction of a landslide model requires proper recognition of landslide geometry, slip surface, deformational structures, soil layering, shear strength parameters, and hydrology (Gallipoli et al. 2000; Ronchetti et al. 2009; Krzeminska et al. 2012; Loke et al. 2013; Perrone et al. 2014; Szokoli et al. 2017; Hu et al. 2017; Dai et al. 2018; Watlet et al. 2018; Carlini et al. 2018). There are several methods for the subsurface modeling and material characterization of landslides, among which geotechnical methods (boreholes, field, and laboratory tests) are widely used because they provide punctual but reliable data about subsurface conditions (Topal and Akin 2009; Suryo 2013; Proutzopoulos et al. 2014; Topsakal and Topal 2015). Despite their reliability, geotechnical methods are costly, time-consuming, and require penetration into the ground. In addition, the data obtained by these methods

✉ Sadegh Rezaei
S_Rezaei1366@yahoo.com

¹ Faculty of Civil Engineering, Babol University of Technology, Shariati Av, P. O. box: 484, Babol, Mazandaran, Iran

² Faculty of Engineering Geology, Golestan University, Shahid Beheshti Av, P. O. box: 155, Gorgan, Golestan, Iran

is related only to a specific point. Subsurface conditions are highly variable, especially in landslide areas; thus, collecting comprehensive data involves drilling several boreholes with appropriate distribution in landslide areas, which is not cost-effective. Therefore, a complementary approach is needed for landslide investigation (Williams and Pratt 1996; Sass et al. 2008; de Bari et al. 2011; Perrone et al. 2014; Yılmaz and Narman 2015; Szokoli et al. 2017; Gullà et al. 2018).

In recent decades, geophysical methods have been widely used in landslide investigations. These methods are applied to determine the thickness of alluvial deposits, shear wave velocity, fundamental frequency, depth of bedrock, groundwater level, slip surface, etc. in landslide areas (Choobbasti et al. 2013; Rezaei and Choobbasti 2014; Akpan et al. 2015; Rezaei et al. 2015; Fressard et al. 2016; Rezaei and Choobbasti 2017a; Rezaei and Choobbasti 2017b; Rezaei et al. 2018). Geophysical methods are fast, low cost, and nondestructive compared to geotechnical methods and they can investigate vast areas; hence, general interest in these methods is increasing (Oh and Sun 2008; Sudha et al. 2009; Siddiqui and Osman 2013; Devi et al. 2017). On the other hand, geophysical methods also have their disadvantages; these methods are indirect and interpreting their results is complex or requires support by complementary geotechnical data. In addition, their accuracy decreases as penetration depth increases and noise negatively affects the results (Hibert et al. 2012; Loke et al. 2013; Capizzi and Martorana 2014; Guerriero et al. 2014; Guerriero et al. 2017). Today, various geophysical methods are employed in landslide characterization, such as seismic refraction, seismic reflection, ambient noise measurement, ground penetrating radar, electromagnetic surveys, and electrical resistivity tomography (ERT).

Among the geophysical methods, ERT is very useful for landslide investigation. ERT measurements involve low weight equipment (as opposed to boring equipment), making handling easy in landslide and distant areas. This method is based on electrical resistivity measurements (Friedel et al. 2006; Grandjean et al. 2011; Capizzi and Martorana 2014; Merritt et al. 2014; Rønning et al. 2014; Ling et al. 2016; Soto et al. 2017; Yannah et al. 2017; Lv et al. 2017; Uhlemann et al. 2018). One-dimensional measurements have limitations and usually do not show horizontal variations of subsurface electrical resistivity. Two-dimensional surveys properly show the vertical and horizontal variations of electrical resistivity. Three-dimensional surveys are time-consuming, expensive, difficult, and usually completed in topographic conditions with a slope of less than 20% (Perrone et al. 2014; Capizzi and Martorana 2014).

Factors, such as the presence of clay, degree of saturation, and the weathering intensity in rocks, affect electrical resistivity; hence, this method is sensitive enough to identify and decipher subsurface structures and geological heterogeneities (Braga et al. 1999; Xu et al. 2016; Kolay et al.

2018). ERT 2D surveys can be used for various types of landslides (translational, rotational, etc.) and geological conditions (rock, soil, and combination of both), giving them a wide range of applications. Previous studies have shown that landslide slip surface geometry and deformational structures can be identified using ERT 2D, and the determination of these properties leads to the comprehensive characterization of a landslide (Loke 2004; De Bari et al. 2011; Merritt et al. 2014).

It should be noted that geophysical methods, such as ERT 2D, are non-unique problems. On the other hand, various geological structures may exhibit similar electrical resistivity, making it difficult to distinguish them. Therefore, geotechnical data is essential to calibrate their results. A combination of geotechnical and geophysical methods reduces the cost of field investigations and the time needed for landslide characterization. Moreover, a greater range of landslide area can be selected for investigation and a more comprehensive examination carried out. In addition, geotechnical data eliminates ambiguities of the geophysical methods. A comprehensive understanding of subsurface conditions of a landslide can be achieved by combining geotechnical methods and ERT surveys (Yılmaz and Narman 2015; Szokoli et al. 2017; Bery and Ismail 2018; Martín-Crespo et al. 2018). In other words, both approaches are essential to complement each other.

We reconstruct the Nargeschal landslide model using 2D ERT completed at five locations, geotechnical, and field data. Especially, collected data allow deciphering of the geological characteristics, the subsurface structure, and longitudinal and cross-sectional geometry and hydrology of the Nargeschal landslide. To obtain the most appropriate array, an ERT measurement is performed in two profiles by WS, Wa, and DD arrays. In addition, the relationship between electrical resistivity and change in the degree of saturation and landslide hydrology is investigated by multiple-measuring in one profile at a different time intervals. Samples are then taken for laboratory tests by drilling six boreholes and two trial pits, and field tests are accomplished. Further, the data necessary for calibration of ERT results is obtained.

Study area

The study area comprises a mountainous village named Nargeschal. The village is located 18 km southwest of Azadshahr City, Golestan Province, Iran, which is approximately at an altitude of 1080 m above sea level (MASL). The deposits in the area are generally made of sandstone, shale, coal shale, marl, clay, and silt. Field investigations show that the surface soil is made of sticky fine-grained clay sediments mainly brown to dark red, giving the impression that

they are the result of decomposition and weathering in shale and marl. The red color results from the presence of iron (Fe). Iron induces matric suction due to cementing action with aluminum oxide and increases the stability of slope in dry seasons. Shear strength declines as the suction decreases in wet seasons, which causes an increase in landslide potential (Senthilkumar et al. 2017).

An investigation into landslide hazard zonation of the Golestan province indicates that this area is located in a very high-risk zone (Pourghasemi et al. 2012). The study demonstrates that the area is located within an old semi-active landslide. Many erosional valleys and slide masses can be observed in the Nargeschal area. Unfortunately, these landslides, which occurred a long time ago, have not been completely investigated. Their principal movement direction is toward the northeast. The depth of the slides sometimes reaches 10 m. These landslides have mainly occurred in the bed or margin of flow pathways passing through the Nargeschal village. Figure 1 presents the location and direction of old landslides around the study area.

The study area has experienced major earthquakes and severe precipitation, so that both factors might have had a great impact on landslides in recent years. On May 29, 2014, a flood occurred in the study area after a heavy precipitation. Three days later, on June 1, 2014, an earthquake, with a magnitude of 3.6 on the Richter scale, occurred 20 km from Nargeschal, and it was associated with multiple aftershocks. On June 4, 2014, three days after these earthquakes, the Nargeschal landslide, which is the topic of this paper, occurred. A large volume of soil was displaced both downstream and upstream of Nargeschal village due to the landslide. After the reactivation of the slide, the village was evacuated and temporary accommodation was provided for the residents in a safe place. The landslide was roughly 750 m in length and its width was up to 80 m in the upstream and 350 m in the downstream. The slope of the area was between 20 and 30°, with a main slip direction at an azimuth of 80°, while the volume of landslide was estimated to be around 2 million m³. Investigations suggest that the earthquake was the main cause of the landslide in Nargeschal, while the

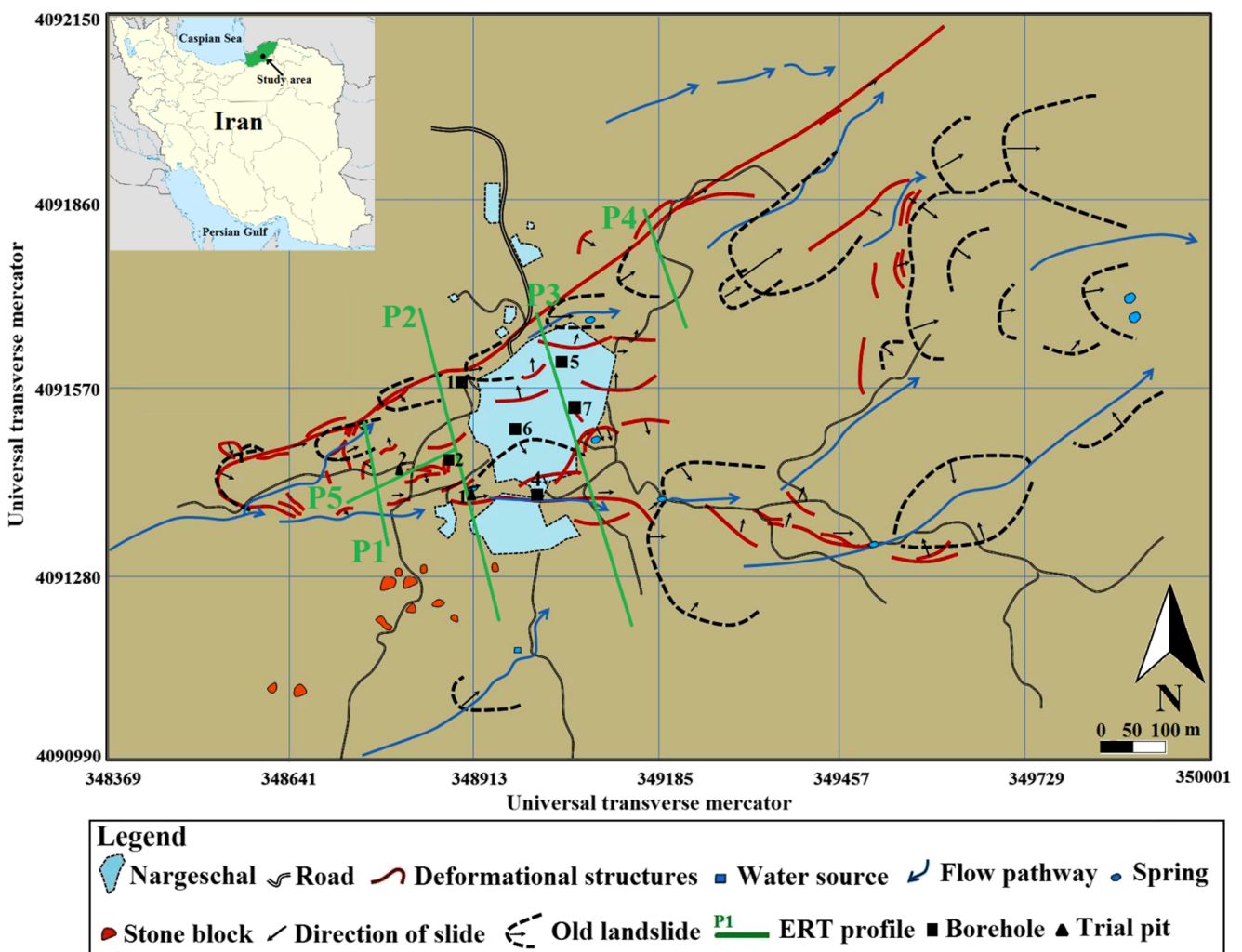


Fig. 1 Landslide map of Nargeschal

heavy precipitation, which occurred before the earthquake, acted as a triggering factor.

Methodology

Subsurface exploration

Six boreholes were completed in order to identify the basal slip surface, collect subsurface data, and calibrate ERT results. Figures 1 and 2 present the location and logs of boreholes, respectively. The standard penetration test (SPT) was performed during boring. Previous studies suggest that slip surface can be identified by the examination of the landslide material stiffness; therefore, it can be detected using SPT-N. Studies by Ahmad et al. (1993), Wei et al. (2008), Topal and Akin (2009), Suryo (2013), Mori et al. (2013), and Topsakal and Topal (2015) may be referred to in this regard. The results of these studies showed that SPT-N has a significant variation around the slip surface.

Two trial pits were also drilled for calibration and reliability of ERT results, as shown in Fig. 1. The drilling of trial pits helped in determining the slip surface. In some situations, trial

pits would be more advantageous than borings. Trial pits can provide data down to 4–5 m below the surface. Unlike borings, the soil can be visually observed from the sides of the trial pit.

Laboratory testing

Laboratory testing is an important element in landslide investigation. Laboratory testing is performed to estimate a slip surface strength that is necessary for the design of a 3D model of landslide. The benefits of laboratory testing include the ability to simulate and control a variety of environmental and/or structural loads, provide fundamental parameters for analytical models, and perform parametric sensitivity studies (Fang 2013).

Disturbed and undisturbed samples were taken from different depths for laboratory tests. Various tests, such as soil classification, sieve analysis, specific gravity, Atterberg limits, moisture content, unit weight, coefficient of permeability, and direct shear tests, were performed on the samples (ASTM D2487, ASTM D422–63, ASTM D854–87, ASTM D4318–87, ASTM D2216–90, ASTM D698–78, ASTM D2454–68, and ASTM D 3080–90).

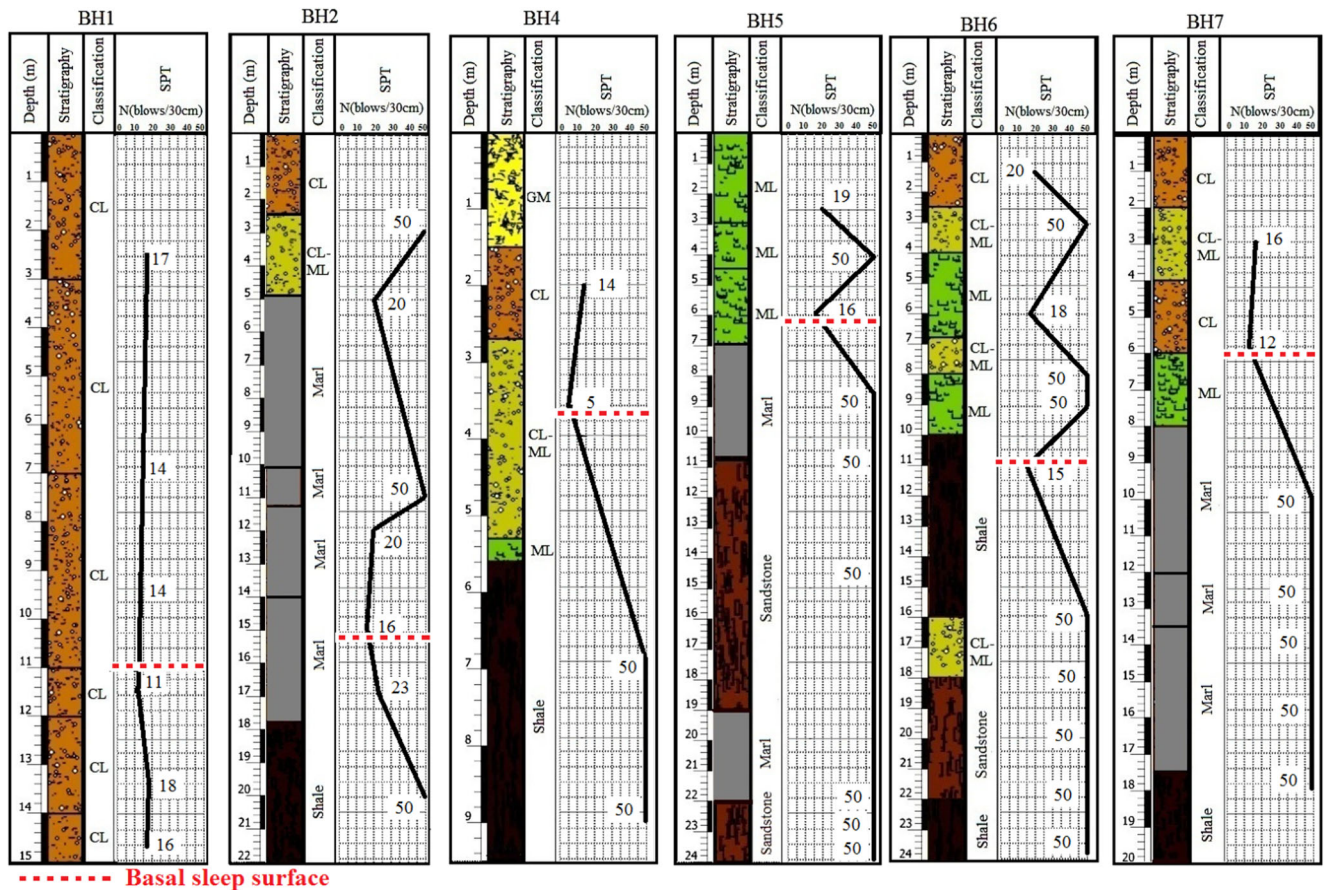


Fig. 2 Logs of boreholes

Field investigations

Field investigations were completed to achieve the following data to support our reconstruction of the landslide model:

1. Determination of the lateral limit of the landslide.
2. Determination of the geometry of slope, such as slope angle, elevation, and run-out distance of the landslide.
3. Identification of coordinates, composition, slope angle, direction, and dimensions of rock outcrops.
4. Identification of old landslides and specification of their geometry.
5. Identification of the expansion, trend, and length of deformational structures in recent landslides.
6. Determination of location of ERT profiles.
7. Analysis of geomorphological parameters.
8. Determination of the location of flow pathways and springs.

ERT survey

The relationship between electrical resistivity (R), current (I), and electrical potential (V) is based on Ohm's law. With the knowledge of the value of I , ΔV , and K (geometric factor, which depends on the type of array), apparent resistivity (ρ_a) of subsurface soil can be calculated using Eq. (1) (Loke et al. 2013).

$$\rho_a = K \frac{\Delta V}{I} \quad (1)$$

Of course, the apparent resistivity is different from the electrical resistivity of a subsurface soil. There is a complicated relationship between electrical and apparent resistivity as an inversion problem, which will be discussed later.

Different arrays are used for ERT and each has its advantages and disadvantages. Field condition, signal strength, sensitivity, and resolution affect the selection of the appropriate array (Perrone et al. 2014; Dostál et al. 2014). Owing to high signal strength, the Wa array is an ideal method in areas having noises, as well as for providing a good vertical resolution. The DD array is a suitable method if good horizontal resolution and suitable data coverage is required. The WS array is also used for horizontal and vertical resolution with good signal strength (Loke 2004; Loke et al. 2013; Perrone et al. 2014).

Perrone et al. (2014), in their comprehensive studies, stated that no review and comparison of different arrays had been done in landslide areas and the array causing the lowest RMSE is usually presented. Their studies showed that DD, Wa, and WS arrays are most commonly used in landslide areas, while other arrays are not often used. In this study, the results of Wa, WS, and DD arrays were thus studied and their efficiency, accuracy, and differences are

evaluated in order to obtain an ideal array for landslide subsurface exploration.

In this study, five ERT profiles were completed for landslide investigation (four profiles normal and one profile parallel to landslide direction). The profiles began outside the landslide area so that the lateral slip surface of the landslide could be detected (e.g., Guerriero et al. 2017). A more appropriate and uniform distribution of profiles was not possible in the study area because of topographical conditions and private occupancy of the land. One profile (P3) for multiple-measurement and two profiles (P2 and P3) for examination of the results of various arrays were selected. Figure 1 presents the location of the profiles and Table 1 presents parameters of their measurements and inversions.

Measurements were performed in profiles P1, P4, and P5 using ABEM Terrameter SAS 4000. These profiles were 190 m in length. However, measurements in profiles P2 and P3 were completed using Geomative-GD10. This device uses multi-core cables and 48 electrodes with a maximum distance of 10 m from each other. This multi-channel system drastically reduces the measurement time. All electrodes are connected to the resistivity meter via multi-core cables. In each measurement, the resistivity meter automatically selects four specific electrodes and measures the apparent resistivity; so this process is repeated several times for different pairs. Initial analysis of the apparent resistivity during measurements indicated good quality of the data. Since the study area had a complex topography, topographic data was collected using a topographic map and GPS and applied in the processing.

The distance between electrodes and topographic data of the profile was introduced to RES2Dinv software in order to calculate electrical resistivity. RES2Dinv software is based on the least squares method and uses the finite element (FE) and finite difference (FD) solutions. It inverts the pseudo-section apparent resistivity to subsurface electrical resistivity distribution using the Quasi-Newton optimization technique (Zarroca et al. 2014; Akpan et al. 2015; Ling et al. 2016; Soto et al. 2017). Given the topography, the software employs a finite element to determine apparent resistivity. It meshes the subsurface space as a large number of rectangular blocks. Given the high variations in resistivity of the ground surface, blocks with widths of half of the unit spacing were used; thus, enhancing the accuracy of the results. The electrical resistivity of these blocks varied in the horizontal and vertical directions but their size and position were constant. The optimization method adjusted the 2D electrical resistivity model by trying to iteratively reduce the difference between the calculated and measured apparent resistivity values. The quality of the inversion process was obtained by examining the root mean square error (RMSE) between the measured and calculated model. Typically, an RMSE less than 5% is considered an

Table 1 Measurement and inversion parameters

Profile name	P1		P2		P3		P4		P5
Electrode array	WS	Wa	WS	DD	Wa	WS	DD	WS	WS
Profile length (m)	190	470	470	470	470	470	470	190	190
Number of iterations	5	4	4	4	4	4	4	4	5
RMSE (%)	3.98	3.40	3.17	3.85	2.96	2.47	4.44	4.01	3.19
Initial damping factor	0.15	0.1	0.1	0.1	0.1	0.1	0.1	0.15	0.15
Increase of damping factor with depth	1.2	1.1	1.1	1.1	1.1	1.1	1.1	1.2	1.2
Vertical to horizontal flatness filter ratio	1	1	1	1	1	1	1	1	1
Forward modeling numerical approach	FE	FE	FE	FE	FE	FE	FE	FE	FE

appropriately inverted model (Loke et al. 2013; Akpan et al. 2015; Yalcinkaya et al. 2016; Devi et al. 2017). In this study, RMSE was less than 5% for all profiles (Table 1).

Multiple ERT surveys

In profile P3, multiple surveys (WS array) at the same location at different times were conducted to verify the accuracy of the results and to study landslide hydrology. Given the previous studies, an attempt was made to make multiple surveys in wet seasons or after a heavy precipitation. The first surveys took place on July 25 and 28, 2017. A heavy precipitation occurred in the study area shortly after the initial survey (on July 31), reaching 85 mm within half an hour, according to the Meteorological Organization in Golestan province, and the precipitation irregularly continued for several days. The precipitation increased groundwater and decreased matric suction and effective stress in the soil, leading to a decline in shear strength. Consequently, changes in landslide hydrology played a key role in the stimulation of landslide and their circumstances should be checked to investigate landslide. Given that electrical resistivity is very dependent on the moisture content of soil, multiple ERT surveys greatly contribute to the characterization of landslide hydrology and mechanism. The multiple surveys took place on August 14. All re-measurement parameters were similar to those of the initial survey.

Results

Landslide depth from boreholes and SPT

Figure 3 illustrates SPT-N variations in the depths for the different boreholes. It was observed that SPT-N shows a significant change in some boreholes. Previous studies demonstrate that the boreholes drilled up to a depth below the slip surface represent such a log. Similar borehole logs can be found in studies by Ahmad et al. (1993), Isik et al. (Işık et al. 2004), Suryo (2013), Crawford et al. (2015), and Topsakal and Topal (2015).

Investigations show that the slip surface has a very low strength compared to its surrounding layers. Accordingly, the slip surface can be observed in the boreholes BH1 at a depth of 11 m, BH2 at depths of 5 and 15 m, BH4 at a depth of 3.5 m, BH5 at a depth of 6 m, BH6 at depths of 6 and 11 m, and BH7 at a depth of 6 m. Two slip surfaces are observed in BH2 and BH6 suggesting that one is probably related to a surface rupture and another to a deeper rupture (basal slip surface). It should be noted that these slip surfaces are detectable by studying the core samples, confirming the SPT-N results. For example, Fig. 4b shows the deformation in the core sample collected from borehole.

Geotechnical characteristics of the landslide material

The results of direct shear test indicate that c values vary from 14 to 75 Kpa, and ϕ values vary from low to 28 degrees in the landslide body. Table 2 presents the geotechnical properties around the slip surface in different boreholes obtained from laboratory tests. Slip surfaces are visible in layers CL, ML, and CL-ML. Also, Fig. 5 shows the results of the Atterberg limits test on slip surface materials. The materials have a low to medium plasticity index.

The results of sieve analysis indicate that the soil has fine-grained particles at the slip surface. The results of the coefficient of permeability also suggest that its values vary between $9.41E-7$ and $3.63E-8$ cm/s in the study area.

Figure 4a shows the slip surface observed in TP1. The stiffer soil under the slip surface is evident during the drilling of trial pits.

Landslide geometry from ERT profiles and field investigations

Figures 6 and 7 shows ERT results for P1, P4, and P5 profiles and different arrays of P2 and P3 profiles, respectively. Figure 8 shows the results of all profiles as a quasi 3D view. Field investigations were conducted with ERT surveys to identify the local conditions. Slip surfaces were identified in different

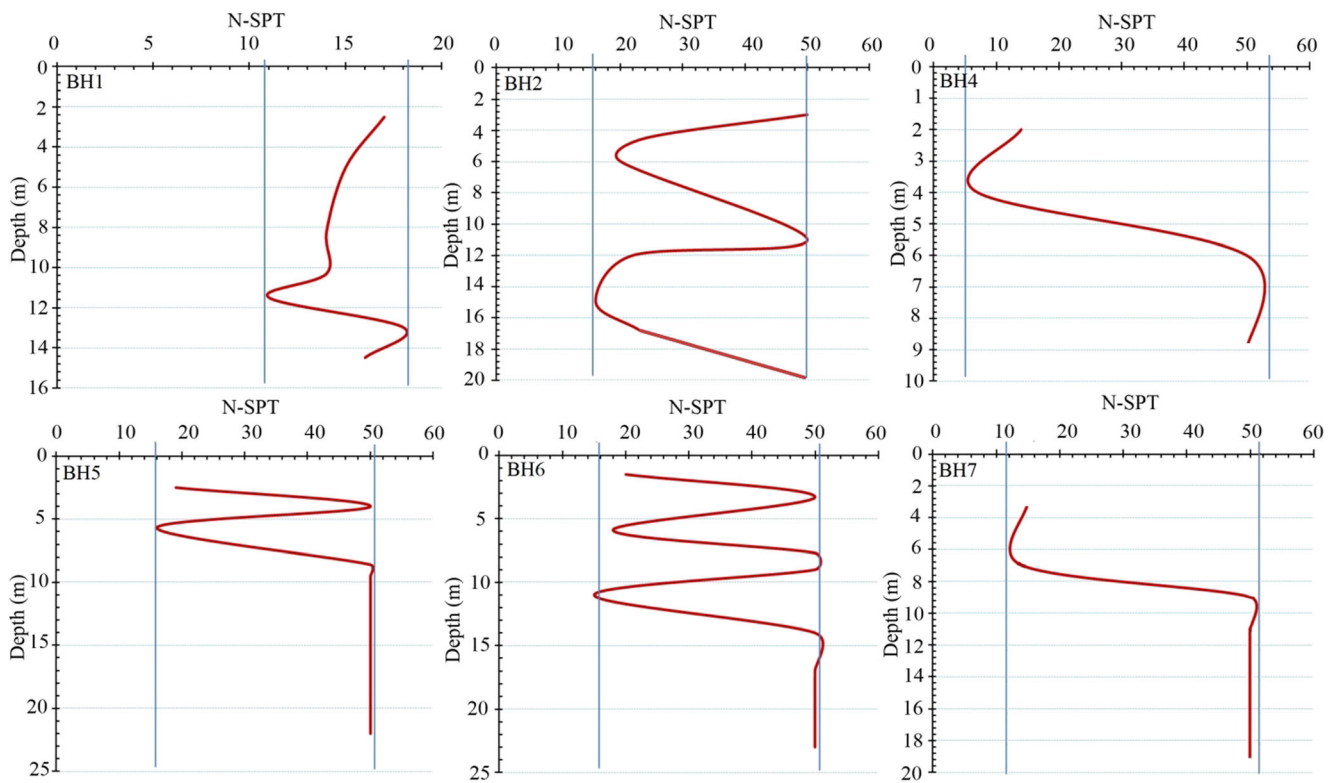


Fig. 3 SPT-N variations in boreholes

profiles using ERT results, geotechnical data, and field investigations (dotted lines in Figs. 6 and 7).

Profile P1 is normal to the landslide direction. The ERT results are consistent with rock outcrop observed in field investigations at the beginning of the profile (at a distance of 35–50 m from the beginning of the profile). In this profile, the lateral limits of the landslide are consistent with the results of field investigations. The slip materials forming the basal shear band are mainly made of clay. Flow pathways located 55 m from the beginning of the profile are properly detectable in ERT results.

Profile P2 is normal to the direction of landslide. All arrays exhibit a region of high electrical resistivity at the

beginning (at a distance of 85–120 m from the beginning of the profile) and the end of the profile (at a distance of 375–405 m from the beginning of the profile), which are detected in field investigations. In this profile, the landslide mass is composed of fine grained material (clay and slit). The depth of the slip surfaces is relatively higher than those observed in profile P1, located upstream of this profile. According to Fig. 1, it is clear that the end of profile P5 meets profile P2 (at a distance of 220 m from the beginning of profile P2). The areas of low electrical resistivity observed at the end of profile P5 are properly represented in all arrays of profile P2. The location of spring at 280 m from the beginning of the profile is well detectable in the results of all arrays.

Profile P3 is normal to the direction of the landslide. All arrays exhibit a region of high electrical resistivity at the beginning and end of the profile. In this profile, the slide masses are composed of fine grained material (clay and silt). The depth of slip surface is relatively greater than those observed in profile P2, which is located upstream of this profile. The flow pathways located 280 m from the beginning of the profile is well defined in the results obtained from all arrays. In addition, the landslide lateral limits in this profile in the Wa and WS arrays are consistent with the results of the field investigations.

Profile P4 is normal to the direction of the landslide. The slip surface can be observed along the profile at varying depths, reaching 25 m at some areas. In this profile, the lateral

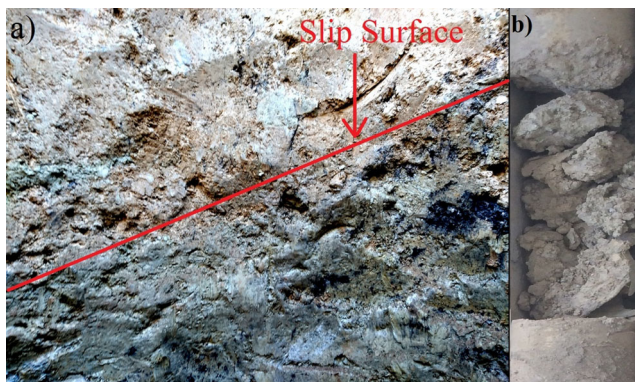


Fig. 4 a) Slip surface observed in TP1 b) Deformation in core sample of borehole

Table 2 Geotechnical properties near the slip surface

Geotechnical characteristics	BH1	BH2	BH3	BH4	BH5	BH6	BH7
Depth of slip surface (m)	11	5	15	3.5	6	6	7
Soil classification	CL	CL-ML	CL	CL-ML	ML	ML	CL
Liquid limit (%)	29	27	33	28	31	30	34
Plastic limit (%)	18	21	19	22	25	24	23
Plastic index (%)	11	6	14	6	6	6	11
Moisture content (%)	21.7	21	18	30	25.3	19	17

limits of the landslide are consistent with the results of the field investigations. The slide materials are primarily composed of clay. The bedrock is clearly identifiable in this profile.

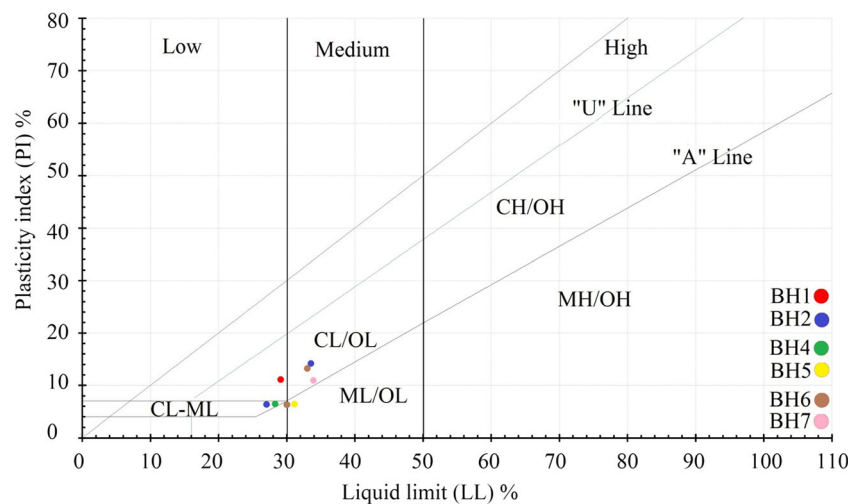
Profile P5 is parallel to the direction of the landslide. A sandstone area with high electrical resistivity is detected at the beginning of profile P5, which is also observed in profile P1. In addition, the end of profile P5 indicates areas of a low electrical resistivity that are similarly detectable by an assessment of profile P2. The rock and stiff soil observed along the profile (at a distance of 110–150 m from beginning of the profile) are consistent with the results of the field investigations. In this profile, the landslide materials are mainly composed of clay and silt.

Landslide hydrology from multiple ERT surveys

Figure 9 shows the changes of electrical resistivity in profile P3 in remeasurements compared to initial survey. In this figure, the results of the initial survey are considered as reference electrical resistivity. It is observed that a large portion of the profile is subject to low changes up to $\pm 2.5\%$. However, an increase by 15% and a decrease by 40% are observed in other areas. Landslide hydrology can be identified by investigating the change of electrical resistivity.

Discussions

Geotechnical analyses indicated that fine-grained soil layers (the main soil type in the study area) are classified as soft to stiff layers based on Federal Highway Administration (FHWA) criteria (Arman et al. 1997). Studies show that the soil has poor shear strength parameters in the slide zone (according to Yalcin (2011) criteria) and this aspect explains the occurrence of landslide in Nargeschal after a relatively small earthquake. The presence of silt increases the value of ϕ . The values of shear strength parameters obtained in this study area are consistent with the values obtained by Yalcin (2011) and Soto et al. (2017), who studied more than 50 and four different landslides, respectively. An investigation into the moisture content and Atterberg limits indicates that the moisture content is very close to the plastic limit. This suggests that the soil is in a plastic form or it becomes soft and plastic due to a slight increase in moisture content, consequently raising its slip potential (Yalcin 2011). These conditions are similar to the geotechnical conditions of the past landslides. Soto et al. (2017) discovered, that in many landslides, the moisture content at the slip surface was very close to the plastic limit. The results of the coefficient of permeability are in accordance with the low permeability of the clay. Studies by Yin et al. (2016) and Soto et al. (2017) showed the coefficient of permeability to be very low and close to impermeable, as obtained in this study.

Fig. 5 Plasticity chart for slip surface materials

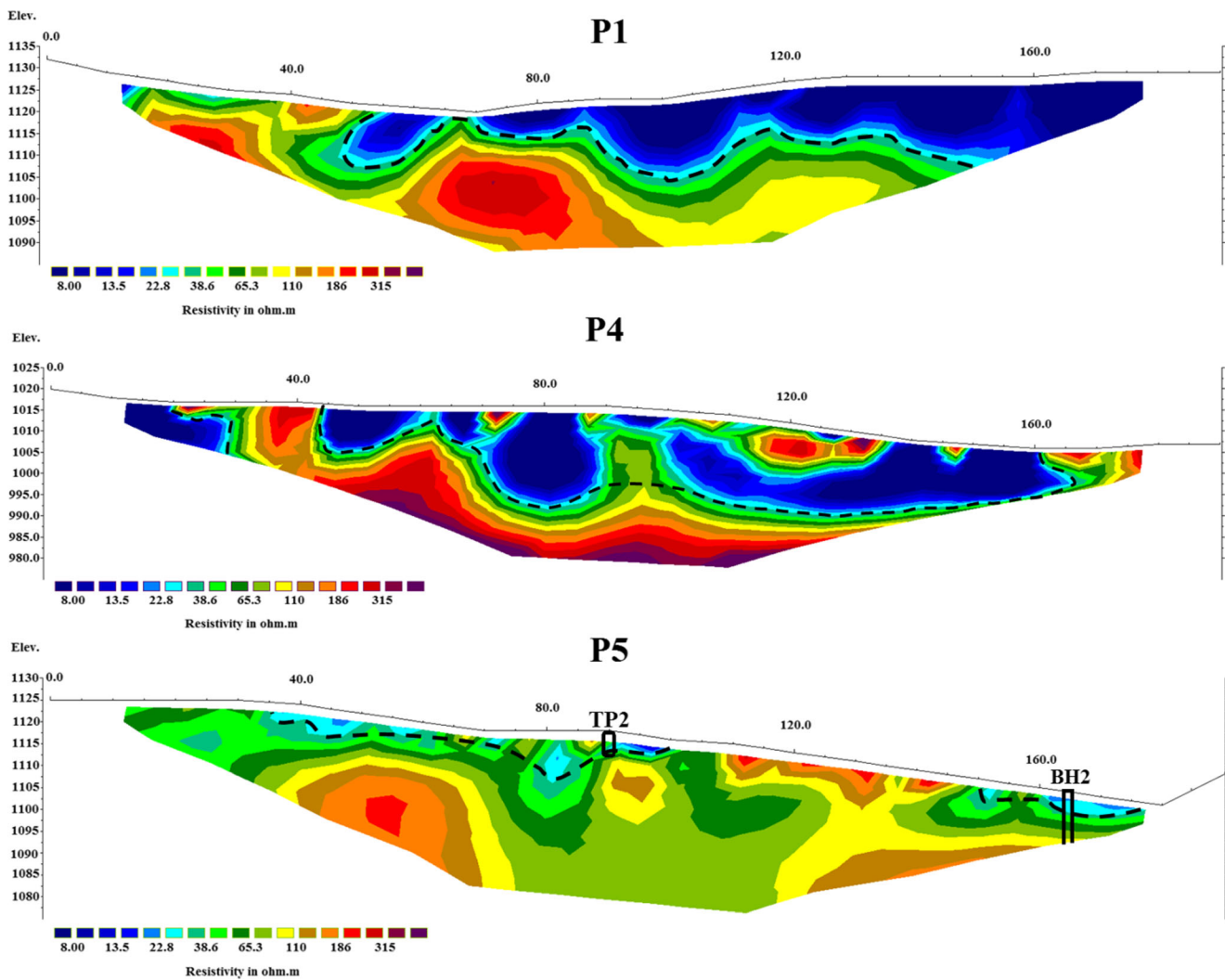


Fig. 6 Inversion results of ERT for P1, P4, and P5 profiles

ERT survey analyses demonstrated that the basal slip surfaces have various depths in different profiles; in P1, for example, the basal slip surface is seen in much of the length of the profile, while it is detected in a small section in profile P5; or the basal slip surface has a low depth in profile P1, while it has a greater depth in profile P3 (This seems reasonable because profile P1 is located in the upstream area of landslide and a shallower slip surface is expected in these areas). The results of Wa and WS arrays are consistent with each other in both profiles P2 and P3. The slip surfaces obtained from these two arrays are approximately the same in terms of position and depth in profiles. Profile P4 is located downstream of the landslide, where slide masses of previous landslides are accumulated, causing heterogeneity within the profile. This is the reason for the scattering of areas of high electrical resistivity amongst areas of low electrical resistivity on the ground surface along the profile. A comparison of the depth of the basal slip surface at the intersection of the profiles (P1 and P5) shows that the results are consistent with each other (Fig. 8).

This indicates the reliability of the measurements and the precision of the inversion process.

Considering the field investigations and a comparison of the ERT results with geological data and logs of boreholes, it can be concluded that high electrical resistivity (more than $186 \Omega\text{-m}$) refers to sandstone and conglomerate; moderate electrical resistivity ($38.6\text{--}186 \Omega\text{-m}$) refers to weathered rock, shale and marl; and low electrical resistivity (less than $30 \Omega\text{-m}$) refers to fine-grained soil, clay, and silt. These intervals are consistent with the results of the previous studies (Loke 2004; Gunn et al. 2015). It must be noted that electrical resistivity variations do not necessarily correspond with the changes in soil layering. In addition, different types of soils and layers can overlap in electrical resistivity intervals. Thin geological layers may not be observed in ERT results (Coşkun et al. 2016). Moreover, no specific range of electrical resistivity can be considered as an indicator of basal slip surface, but it rather takes different values in different sites. The points explained above should be considered in the interpretation of the

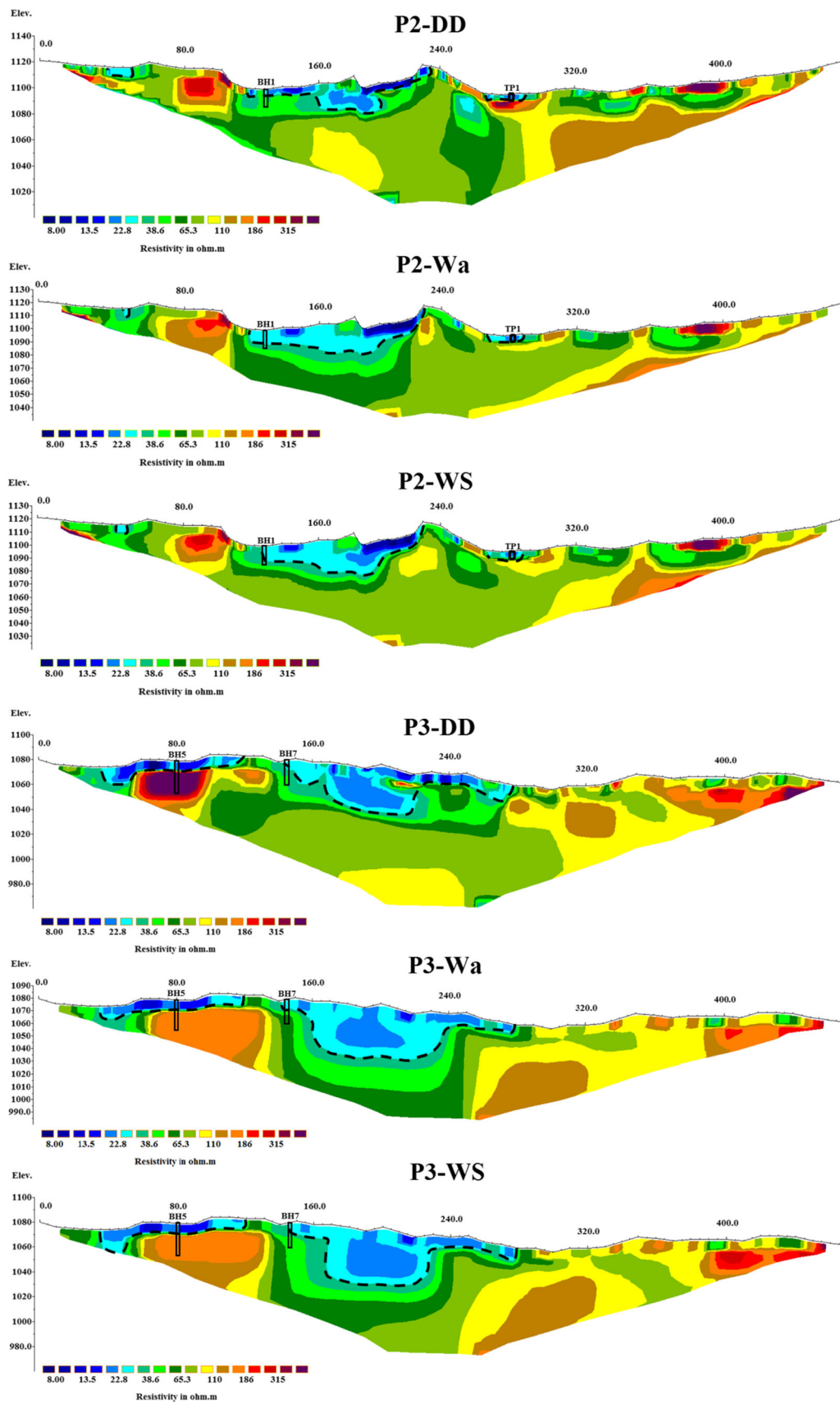


Fig. 7 Inversion results of ERT for different arrays in P2 and P3 profiles

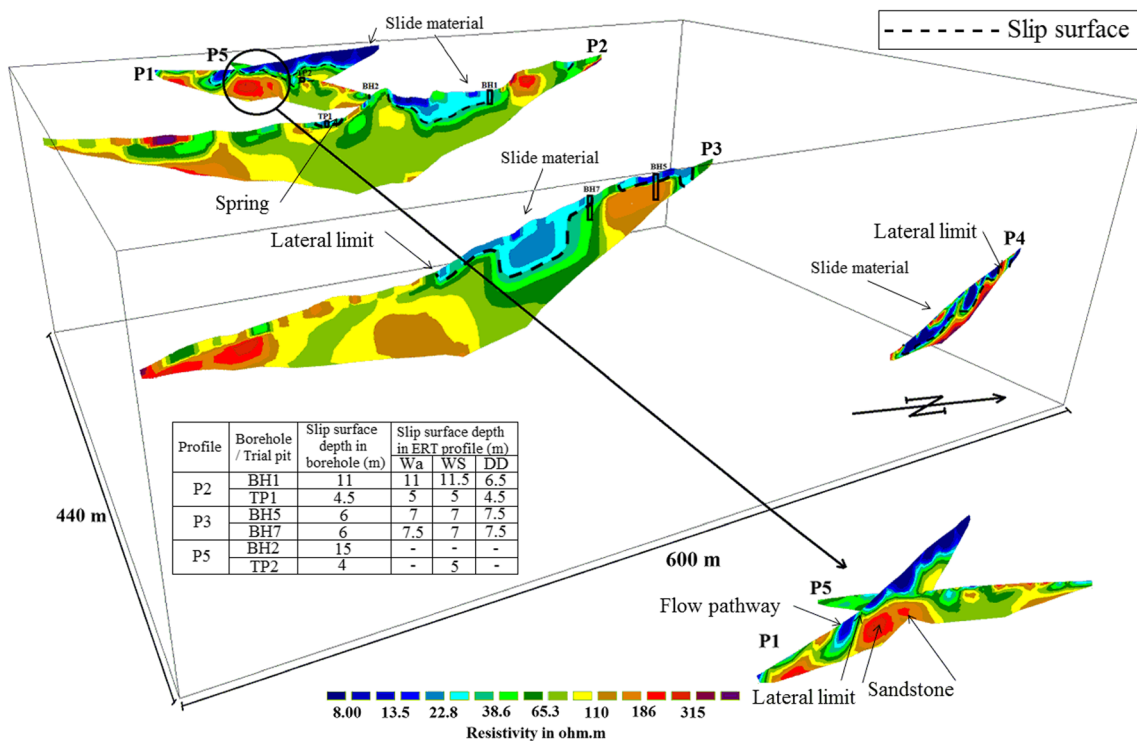


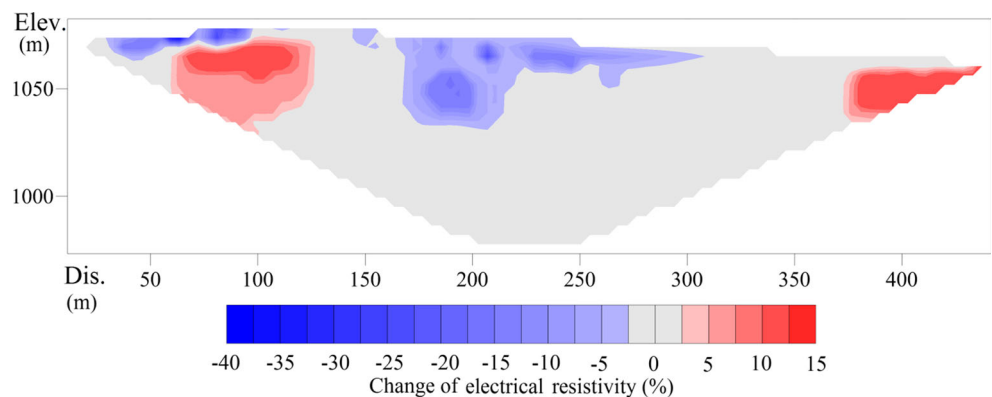
Fig. 8 Inversion results of ERT in all profiles in a quasi 3D view

results, as the electrical resistivity intervals given above refer to approximate values. An exact comment about subsurface changes only relies on a comparison of ERT results with the geological and geotechnical data.

The combination of geotechnical and geophysical methods is essential. Geotechnical data is used for calibration and reliability. Borehole BH1 is located 130 m from the beginning of profile P2. The slip surface is observed at a depth of 11 m in this borehole (Fig. 2). From the ERT results, Wa and WS arrays accurately detect this slip surface. However, the DD array shows the slip surface at a depth of 6.5 m. According to previous studies, the DD array is sometimes not able to recognize deformational structures at high distances between current and potential electrodes, and this probably leads to a miscalculation of the slip sur-

face (Loke 2004). It should be noted that variations of electrical resistivity of profile P2 in depth are precisely consistent with changes in soil characteristics in this borehole. Borehole BH2 is located 165 m from the beginning of profile P5. In this borehole, two slip surfaces exist at depths of 5 and 15 m (Fig. 2). No basal slip surface (i.e., the lower boundary of the sliding mass) is observed at a depth of 15 m in the ERT results because the penetration depth of this method is insufficient. In cases where ERT methods are inadequate for basal slip surface detection, geotechnical data and field investigations were used. You might interpret landslide basal slip surface geometry from the distribution of surface displacement or structures (Guerriero et al. 2014; Aryal et al. 2015). Therefore, the combination of geotechnical and geophysical methods is essential. The penetration

Fig. 9 Electrical resistivity changes in profile P3 in remeasurements compared to initial survey



depth and resolution can be enhanced by increasing the profile length, decreasing the distance between electrodes, and changing the type of arrays. Borehole BH5 is located 80 m from the beginning of profile P3. The slip surface is observed at a depth of 6 m in this borehole (Fig. 2). ERT results demonstrate that all arrays accurately detect this slip surface (at a depth of 7–7.5 m). In addition, variations of electrical resistivity of profile P3 in depth are precisely consistent with changes in soil characteristics in this borehole. Hence, variations in materials from fine grains to marl and then sandstone is evidently seen in the ERT results by increasing electrical resistivity. Borehole BH7 is also located 145 m from the beginning of profile P3. The slip surface is observed at a depth of 6 m in this borehole (Fig. 2). ERT results demonstrate that all arrays accurately detect this slip surface (at a depth of 7–7.5 m). In addition to the slip surface, variations of electrical resistivity of profile P3 in depth are precisely consistent with changes in soil characteristics in this borehole. Hence, a variation of materials from fine grains to marl is obvious in the ERT results due to increasing electrical resistivity. Trial pit TP1 is located at a distance of 285 m from the beginning of profile P2. The slip surface is visible at a depth of 4.5 m within this trial pit, indicating that the ERT measurements obtained from different arrays approximately show the same depth. Trial pit TP2 is located 90 m from the beginning of profile P5. In this trial pit, the slip surface is observed at a depth of 4 m, which is acceptably consistent with the ERT results (the slip surface can be seen at a depth of 5 m).

Given the results of this study, it is observed that the array offering the lowest RMSE is not necessarily the best one. A relative assessment of subsurface data is required to select the most appropriate array, and this matter indicates the necessity of a combination of both geotechnical and geophysical methods. In general, it is recommended to measure different arrays and interpret the subsurface conditions by comparing the results and geotechnical data of the area. If it is not possible to measure the electrical resistivity in different arrays, then it is first necessary to identify the type of subsurface structure (horizontal or vertical) through investigating geological data and geotechnical boreholes and, then, select the appropriate array. The results suggest that the DD array is generally recommended if electrical resistivity changes near the ground surface are high and good vertical resolutions are needed. The Wa array is recommended if the noise level of the study area is high and a good horizontal resolution is required. The WS array is recommended if no initial data about subsurface conditions is available, horizontal and vertical resolution is needed or it is possible to measure only one array.

The result of multiple ERT survey indicates that the areas of low electrical resistivity are mainly shallow and fine-grained clay layers. This is due to an increase in moisture content and saturation of the soil in these areas. In some places, electrical

resistivity increased up to 15%. These areas also show a high value in initial survey which were considered as sandstone layers. Such conditions are similarly observed in studies by Ling et al. (2016) and Xuo et al. (Xu et al. 2016). They also mentioned increased moisture content and drainage as reasons for a decrease and an increase in electrical resistivity, respectively. The electrical resistivity of the areas considered as slip surface and slide materials in the initial survey was mainly decreased, indicating the reliability of the slip surface detected in Fig. 7. Multiple ERT surveys are very useful. It helps in assessing the reliability of the initial measurement results and accurate determination of slide materials, slip surfaces, and landslide hydrology. These multiple surveys are strongly recommended if the conditions and the budget for remeasurement at different time intervals (time lapse ERT) are available.

The study of the Nargeschal landslide is accomplished through investigation and comparison of the geotechnical and geophysical methods. ERT results combined with field data and geotechnical analysis accurately depict the landslide geometry, lateral limits, slip surface depth, geology, and hydrology. A ground model was developed based on ERT survey, field investigations, and thorough interpretation of results from core logging, geotechnical testing, and laboratory analysis of core samples (Fig. 8). By investigating the quasi 3D model of the landslide, it is evident that the slip surface depth increases as one moves from upstream to P3 profile, while it decreases downstream of the landslide (P4 profile). The presence of fine grained material and groundwater flows impose significant impacts on the occurrence of landslide, so that in nearly all profiles, the slide masses are composed of fine grained material (clay and silt). The weak layers overlaying the stiff layers represent another factor contributing to high landslide potential across the study area; this is well evident at borehole BH5. Flow pathways and springs also play significant roles in the occurrence of landslide and development of unstable areas; this can be clearly observed in Fig. 8.

Given the 3D model of landslide, the following can be introduced as factors contributing to the occurrence of the Nargeschal landslide: complex topography, low shear strength fine-grained materials, heavy precipitation, and earthquake. Following Glade and Crozier (2005), four groups of factors may be involved in the development of landslides. Predisposing factors are static, inherent factors that favor slope instability. In the case of the Nargeschal landslide, the main predisposing factors correspond to topography condition (the slope of the study area was between 20 and 30°). Preparatory factors are dynamic factors that may shift a slope from a stable to a marginally stable state, without initiating any movement. Probably, the most significant preparatory factors involved in the development of the Nargeschal landslide include the progressive reduction in the shear strength of the sediments enhanced by focused groundwater flows. The June 1, 2014 earthquake was most likely the trigger factor for this landslide.

Severe precipitation events might be considered as an additional triggering factor. The Nargeschal landslide was triggered six days after precipitation of 130 mm during 24 h. The potential of landslide increases in wet seasons, as indicated by investigating the results of the multiple ERT surveys. Marginal stability conditions can be expected during dry season. The integration of ERT survey, geotechnical data, and field investigation allowed the characterization of the Nargeschal landslide and reconstructing its mechanism and condition factor.

Improvement and stabilization of soil is essential to cope with the damaging effects of landslide and reduce casualties and financial losses caused by this natural hazard. There are various methods for soil improvement that require basic data, such as soil type, depth of improvement, budget of the project, etc. The interpretation of the result, in other words the landslide model, can be used as a basis for planning mitigation measurements. For example, the landslide geometry, soil type, depth of slip surface, and groundwater level can be reconstructed by using geotechnical data and ERT results, and the most ideal and economical method of soil improvement can be selected using this data. This is the reason why the goal of this paper should be the reconstruction of a landslide model.

Conclusions

In this study, ERT surveys, geotechnical and field methods were used to study the Nargeschal landslide. The soil properties (grain size, unit weight, Atterberg limits, moisture content, permeability, shear strength parameters, etc.) were identified in different areas by drilling six boreholes and two trial pits, taking disturbed and undisturbed samples, and performing laboratory tests. The investigation of these properties and their changes in depth greatly helped in determining the geological characteristics and the depth and geometry of the slip surfaces. The results of geotechnical investigations showed that the landslide material had moisture content very close to the plastic limit, with a higher clay fraction and low shear strength at the slip surface. Moreover, slip surfaces were identified in boreholes by performing SPT and investigating the variations of the SPT-N in the study area. These estimated slip surfaces were properly consistent with the core sample taken in the boreholes. Field investigations were also conducted in addition to field and laboratory tests. Field investigations were used to determine landslide characteristics, rock outcrops, surface soil types, deformational structures, and the location of springs and flow pathways. These data were employed for the calibration and the reliability of the ERT results.

In addition to the geotechnical and field methods, the ERT survey was carried out in five profiles to reconstruct the landslide model. The results show that a multi method approach allows identifying landslide geometry, lateral limits, landslide hydrology, and slip surface with accuracy. The electrical

resistivity variations in depth were consistent with changes in the soil characteristics within the boreholes and the trial pits. This indicates the precision of measurement and the inversion process as well as the importance of geotechnical data.

The results of the WS and the Wa arrays are consistent with each other. The DD array is not accurate enough to determine the slip surface and the lateral limits in some cases, but instead it performs more successfully in identifying structures with high electrical resistivity near the ground. Given the results, considering that the array with the lowest RMSE as the final answer is not recommended, using different arrays and interpreting the subsurface conditions by comparing their results and geotechnical data is preferred.

The results of multiple surveys indicate that they are very useful to verify the results of the initial survey and accurately determine the slide materials, slip surfaces, and landslide hydrology. The electrical resistivity changes in remeasurements compared to the initial survey suggests that after severe precipitation, the moisture content increases immediately above the slip surface and the landslide areas, which are mainly composed of clay and, consequently, their electrical resistivity decreases.

A ground model was developed based on ERT survey, field investigations, and thorough interpretation of results from core logging, geotechnical testing, and laboratory analysis of core samples. The integration of the mentioned methods allowed the characterization of the Nargeschal landslide and reconstructing of its mechanism and condition factor. Given the 3D model of landslide, the following can be introduced as factors contributing to the occurrence of the Nargeschal landslide: extreme topography, low shear strength fine-grained materials, heavy precipitation, and earthquake.

Acknowledgements The authors are thankful to the reviewers for constructive comments and their valuable suggestion which helped us to improve the manuscript.

References

- Ahmad R, Earle AH, Hugues P, Maharaj R, Robinson E (1993) Landslide damage to the board river water supply pipeline, Bromley hill, Jamaica: case study of a landslide caused by hurricane Gilbert. *B Int Assoc Eng Geol* 47:59–70
- Akpan AE, Ilori AO, Essien NU (2015) Geophysical investigation of Obot Ekpo landslide site, Cross River state. *Nigeria J Afr Earth Sci* 109:154–167
- Arman A, Samtani N, Castelli R, Munfakh G (1997) Geotechnical and foundation engineering, module 1–subsurface investigations. Publication No FHWA NHI-97:21
- Aryal A, Brooks BA, Reid ME (2015) Landslide subsurface slip geometry inferred from 3-D surface displacement fields. *Geophys Res Lett* 42(5):1411–1417
- Bery AA, Ismail NEH (2018) Empirical correlation between electrical resistivity and engineering properties of soils. *Soil Mech Found Eng* 54(6):425–429

- Braga AC, Malagutti FW, Dourado JC, Chang HK (1999) Correlation of electrical resistivity and induced polarization data with geotechnical survey standard penetration test measurements. *J Environ Eng Geoph* 4:123–130
- Capizzi P, Martorana R (2014) Integration of constrained electrical and seismic tomographies to study the landslide affecting the cathedral of Agrigento. *J Geophys Eng* 11(4):045009
- Carlini M, Chelli A, Francese R, Giacomelli S, Giorgi M, Quagliarini A, Carpena A, Tellini C (2018) Landslides types controlled by tectonics-induced evolution of valley slopes (northern Apennines, Italy). *Landslides* 15(2):283–296
- Choobbasti AJ, Rezaei S, Farrokhzad F (2013) Evaluation of site response characteristics using microtremors. *Gradev* 65:731–741
- Coşkun N, Çakır Ö, Erduran M, Kutlu YA, Çetiner ZS (2016) A potential landslide area investigated by 2.5 D electrical resistivity tomography: case study from Çanakkale, Turkey. *Arab J Geosci*. <https://doi.org/10.1007/s12517-015-2026-x>
- Crawford MM, Zhu J, Webb SE (2015) Geologic, geotechnical, and geophysical investigation of a shallow landslide. *Eastern Kentucky Environ Eng Geosci* 21:181–195
- Dai Z, Wang F, Cheng Q, Wang Y, Yang H, Lin Q, Kongming Y, Feicheng L, Li K (2018) A giant historical landslide on the eastern margin of the Tibetan plateau. *B Eng Geol Environ*. <https://doi.org/10.1007/s10064-017-1226-x>
- De Bari C, Lapenna V, Perrone A, Puglisi C, Sdao F (2011) Digital photogrammetric analysis and electrical resistivity tomography for investigating the Picerno landslide (Basilicata region, southern Italy). *Geomorphology* 133:34–46
- Devi A, Israil M, Anbalagan R, Gupta PK (2017) Subsurface soil characterization using geoelectrical and geotechnical investigations at a bridge site in Uttarakhand Himalayan region. *J Appl Geophys* 144:78–85
- Dostál I, Putiška R, Kušnirák D (2014) Determination of shear surface of landslides using electrical resistivity tomography. *Contr Geophys Geod* 44:133–147
- Fang HY (2013) *Foundation engineering handbook*. Springer, New York
- Fressard M, Maquaire O, Thiery Y, Davidson R, Lissak C (2016) Multi-method characterisation of an active landslide: case study in the pays d'Auge plateau (Normandy, France). *Geomorphology* 270:22–39
- Friedel S, Thielen A, Springman SM (2006) Investigation of a slope endangered by rainfall-induced landslides using 3D resistivity tomography and geotechnical testing. *J Appl Geophys* 60:100–114
- Gallipoli M, Lapenna V, Lorenzo P, Mucciarelli M, Perrone A, Piscitelli S, Sdao F (2000) Comparison of geological and geophysical prospecting techniques in the study of a landslide in southern Italy. *J Environ Eng Geoph* 4:117–128
- Glade T, Crozier MJ (2005) The nature of landslide hazard impact. In: Glade T, Anderson M, Crozier M (eds) *Landslide hazard and risk*. Wiley, Chichester, pp 43–74
- Grandjean G, Gourry JC, Sanchez O, Bitri A, Garambois S (2011) Structural study of the Ballandaz landslide (French alps) using geophysical imagery. *J Appl Geophys* 75(3):531–542
- Guerrero L, Coe JA, Revellino P, Grelle G, Pinto F, Guadagno FM (2014) Influence of slip-surface geometry on earth-flow deformation, Montaguto earth flow, southern Italy. *Geomorphology* 219:285–305
- Guerrero L, Revellino P, Luongo A, Focareta M, Grelle G, Guadagno FM (2016) The mount Pizzuto earth flow: deformational pattern and recent thrusting evolution. *J Maps* 12(5):1187–1194
- Guerrero L, Bertello L, Cardozo N, Berti M, Grelle G, Revellino P (2017) Unsteady sediment discharge in earth flows: a case study from the mount Pizzuto earth flow, southern Italy. *Geomorphology* 295:260–284
- Gullà G, Aceto L, Antronico L, Borrelli L, Coscarelli R, Perri F (2018) A smart geotechnical model in emergency conditions: a case study of a medium-deep landslide in southern Italy. *Eng Geol* 234:138–152
- Gunn DA, Chambers JE, Uhlemann S, Wilkinson PB, Meldrum PI, Dijkstra TA, Haslam E, Kirkham M, Wragg J, Holyoake S, Hughes PN (2015) Moisture monitoring in clay embankments using electrical resistivity tomography. *Constr Build Mater* 92:82–94
- Hibert C, Grandjean G, Bitri A, Travelletti J, Malet JP (2012) Characterizing landslides through geophysical data fusion: example of the La Valette landslide (France). *Eng Geol* 128:23–29
- Hu J, Li S, Li L, Shi S, Zhou Z, Liu H, He P (2017) Field, experimental, and numerical investigation of a rockfall above a tunnel portal in southwestern China. *B Eng Geol Environ*. <https://doi.org/10.1007/s10064-017-1152-y>
- İşık NS, Doyuran V, Ulusay R (2004) Assessment of a coastal landslide subjected to building loads at Sinop, Black Sea region, Turkey, and stabilization measures. *Eng Geol* 75:69–88
- Krzeminska DM, Bogaard TA, Van Asch TW, Van Beek LPH (2012) A conceptual model of the hydrological influence of fissures on landslide activity. *Hydrol Earth Syst Sc* 16(6):1561–1576
- Kolay PK, Burra SG, Kumar S (2018) Effect of salt and NAPL on electrical resistivity of fine-grained soil-sand mixtures. *Int J Geotech Eng* 12(1):13–19
- Kramer SL (1996) *Geotechnical earthquake engineering*. Prentice Hall, Upper Saddle River
- Ling C, Xu Q, Zhang Q, Ran J, Lv H (2016) Application of electrical resistivity tomography for investigating the internal structure of a translational landslide and characterizing its groundwater circulation (Kualiangzi landslide, Southwest China). *J Appl Geophys* 131:154–162
- Loke MH (2004) Tutorial: 2-D and 3-D electrical imaging surveys. Geotomo software, Penang, Malaysia
- Loke MH, Chambers JE, Rucker DF, Kuras O, Wilkinson PB (2013) Recent developments in the direct-current geoelectrical imaging method. *J Appl Geophys* 95:135–156
- Lv H, Ling C, Hu BX, Ran J, Zheng Y, Xu Q, Tong J (2017) Characterizing groundwater flow in a translational rock landslide of southwestern China. *B Eng Geol Environ*. <https://doi.org/10.1007/s10064-017-1212-3>
- Martín-Crespo T, Gómez-Ortiz D, Martín-Velázquez S, Martínez-Pagán P, De Ignacio C, Lillo J, Faz Á (2018) Geoenvironmental characterization of unstable abandoned mine tailings combining geophysical and geochemical methods (Cartagena-La Union district, Spain). *Eng Geol* 232:135–146
- Merritt AJ, Chambers JE, Murphy W, Wilkinson PB, West LJ, Gunn DA, Meldrum PI, Kirkham M, Dixon N (2014) 3D ground model development for an active landslide in Lias mudrocks using geophysical, remote sensing and geotechnical methods. *Landslides* 11:537–550
- Mori T, Tobita Y, Okimura T (2013) Damages of hillside embankments in Sendai City during the 2011 great East Japan earthquake. In: Ugai K, Yagi H, Wakai A (eds) *Earthquake-induced landslides*, 1st edn. Springer, Berlin, pp 261–273
- Oh S, Sun CG (2008) Combined analysis of electrical resistivity and geotechnical SPT blow counts for the safety assessment of fill dam. *Environ Geol* 54:31–42
- Perrone A, Lapenna V, Piscitelli S (2014) Electrical resistivity tomography technique for landslide investigation: a review. *Earth-Sci Rev* 135:65–82
- Pourghasemi HR, Moradi HR, Mohammadi M, Pradhan B, Mostafazadeh R, Goli Jirandeh A (2012) Landslide hazard assessment using remote sensing data, GIS and weights-of-evidence model (south of Golestan Province, Iran). *Asia Pacific Conf Environ Sci Technol, Adv Biomed Eng* 6:30–36
- Prountzopoulos G, Fortsakis P, Seferoglou K, Chrysochoidis F, Vassilopoulou I, Perleros V (2014) Assessment of failure mechanism and rehabilitation of a landslide within Marly formations in NW Greece: from the site investigation to the geotechnical design. *Geotech Geol Eng* 32:1485–1502

- Rezaei S, Choobbasti AJ (2014) Liquefaction assessment using microtremor measurement, conventional method and artificial neural network (case study: Babol, Iran). *Front Struct Civ Eng* 8(3):292–307
- Rezaei S, Choobbasti AJ, Soleimani Kutanaei S (2015) Site effect assessment using microtremor measurement, equivalent linear method and artificial neural network (case study: Babol, Iran). *Arab J Geosci* 8: 1453–1466
- Rezaei S, Choobbasti AJ (2017a) Application of microtremor measurements to a site effect study. *Earthq Sci*. <https://doi.org/10.1007/s11589-017-0187-2>
- Rezaei S, Choobbasti AJ (2017b) Evaluation of local site effect from microtremor measurements in Babol city, Iran. *J Seismol*. <https://doi.org/10.1007/s10950-017-9718-5>
- Rezaei S, Shooshpasha I, Rezaei H (2018) Evaluation of landslides using ambient noise measurements (case study: Nargeschal landslide). *Int J of Geotech Eng*. <https://doi.org/10.1080/19386362.2018.1431354>
- Ronchetti F, Borgatti L, Cervi F, Gorgoni C, Piccinini L, Vincenzi V, Corsini A (2009) Groundwater processes in a complex landslide, northern Apennines, Italy. *Nat Hazard Earth Sys* 9(3):895–904
- Rønning JS, Ganerød GV, Dalsegg E, Reiser F (2014) Resistivity mapping as a tool for identification and characterisation of weakness zones in crystalline bedrock: definition and testing of an interpretational model. *B Eng Geol Environ* 73:1225–1244
- Sass O, Bell R, Glade T (2008) Comparison of GPR, 2D-resistivity and traditional techniques for the subsurface exploration of the Öschingen landslide, Swabian Alb (Germany). *Geomorphology* 93(1):89–103
- Senthilkumar V, Chandrasekaran SS, Maji VB (2017) Geotechnical characterization and analysis of rainfall—induced 2009 landslide at Marappalam area of Nilgiris district, Tamil Nadu state, India. *Landslides*. <https://doi.org/10.1007/s10346-017-0839-2>
- Siddiqui FI, Osman SBABS (2013) Simple and multiple regression models for relationship between electrical resistivity and various soil properties for soil characterization. *Environ Earth Sci* 70:259–267
- Soto J, Galve JP, Palenzuela JA, Azañón JM, Tamay J, Irigaray C (2017) A multi-method approach for the characterization of landslides in an intramontane basin in the Andes (Loja, Ecuador). *Landslides*. <https://doi.org/10.1007/s10346-017-0830-y>
- Sudha K, Israil M, Mittal S, Rai J (2009) Soil characterization using electrical resistivity tomography and geotechnical investigations. *J Appl Geophys* 67:74–79
- Suryo EA (2013) Real-time prediction of rainfall induced instability of residual soil slopes associated with deep cracks. Doctoral dissertation, Queensland University of Technology
- Szokoli K, Szarka L, Metwaly M, Kalmár J, Prácsér E, Szalai S (2017) Characterisation of a landslide by its fracture system using electric resistivity tomography and pressure probe methods. *Acta Geod Geophys*. <https://doi.org/10.1007/s40328-017-0199-3>
- Topal T, Akin M (2009) Geotechnical assessment of a landslide along a natural gas pipeline for possible remediations (Karacabey-Turkey). *Environ Geol* 57:611–620
- Topsakal E, Topal T (2015) Slope stability assessment of a re-activated landslide on the Artvin-Savsat junction of a provincial road in Meydancik, Turkey. *Arab J Geosci* 8:1769–1786
- Uhlemann S, Wilkinson PB, Maurer H, Wagner FM, Johnson TC, Chambers JE (2018) Optimized survey design for electrical resistivity tomography: combined optimization of measurement configuration and electrode placement. *Geophys J Int*. <https://doi.org/10.1093/gji/ggy128>
- Wattlet A, Kaufmann O, Triantafyllou A, Poulain A, Chambers JE, Meldrum PI, Wilkinson PB, Hallet V, Quinif Y, Van Ruymbeke M, Van Camp M (2018) Imaging groundwater infiltration dynamics in the karst vadose zone with long-term ERT monitoring. *Hydrol Earth Syst Sc* 22(2):1563–1592
- Wei Z, Yin G, Wan L, Shen L (2008) Case history of controlling a landslide at Panluo open-pit mine in China. *Environ Geol* 54:699–709
- Williams RA, Pratt TL (1996) Detection of the base of Slumgullion landslide, Colorado, by seismic reflection. In: Varied DJ, Savage WZ (ed) *The Slumgullion earth flow: a large-scale natural laboratory*. US geological survey, Denver, pp 77–83
- Xu D, Hu XY, Shan CL, Li RH (2016) Landslide monitoring in southwestern China via time-lapse electrical resistivity tomography. *Appl Geophys* 13:1–12
- Yalcin A (2011) A geotechnical study on the landslides in the Trabzon Province, NE, Turkey. *Appl Clay Sci* 52:11–19
- Yalcinkaya E, Alp H, Ozel O, Gorgun E, Martino S, Lenti L, Bourdeau C, Bigarre P, Coccia S (2016) Near-surface geophysical methods for investigating the Buyukcekmece landslide in Istanbul, Turkey. *J Appl Geophys* 134:23–35
- Yannah M, Martens K, Van Camp M, Walraevens K (2017) Geophysical exploration of an old dumpsite in the perspective of enhanced landfill mining in Kermt area, Belgium. *B Eng Geol Environ*. <https://doi.org/10.1007/s10064-017-1169-2>
- Yılmaz S, Narman C (2015) 2-D electrical resistivity imaging for investigating an active landslide along a roadway in Burdur region, southern Turkey. *Arab J Geosci* 8:3343–3349
- Yin Y, Li B, Wang W, Zhan L, Xue Q, Gao Y, Zhang N, Chen H, Liu T, Li A (2016) Mechanism of the December 2015 catastrophic landslide at the Shenzhen landfill and controlling geotechnical risks of urbanization. *Engineering* 2:230–249
- Zarroca M, Linares R, Roqué C, Rosell J, Gutiérrez F (2014) Integrated geophysical and morphostratigraphic approach to investigate a coseismic (?) translational slide responsible for the destruction of the Montclús village (Spanish Pyrenees). *Landslides* 11:655–671